Monthly Notices of the ROYAL ASTRONOMICAL SOCIETY

MNRAS **524,** 6149–6158 (2023)
Advance Access publication 2023 July 26

https://doi.org/10.1093/mnras/stad2242

Hubble Space Telescope survey of Magellanic Cloud star clusters: UV-dim stars in young clusters

A. P. Milone [1,2★] G. Cordoni [2] A. F. Marino [2,3] F. Muratore,[1] F. D'Antona [4] M. Di Criscienzo,[4] E. Dondoglio,[1] E. P. Lagioia [1] M. V. Legnardi [1] A. Mohandasan,[1] T. Ziliotto,[1] F. Dell'Agli [1] M. Tailo [5] and P. Ventura [4]

[1]*Dipartimento di Fisica e Astronomia 'Galileo Galilei', Univ. di Padova, Vicolo dell'Osservatorio 3, I-35122 Padova, Italy*
[2]*Istituto Nazionale di Astrofisica – Osservatorio Astronomico di Padova, Vicolo dell'Osservatorio 5, I-35122 Padova, Italy*
[3]*Istituto Nazionale di Astrofisica – Osservatorio Astrofisico di Arcetri, Largo Enrico Fermi 5, I-50125 Firenze, Italy*
[4]*INAF – Osservatorio Astronomico di Roma, Via Frascati 33, I-00040 Monte Porzio Catone, Roma, Italy*
[5]*Dipartimento di Fisica e Astronomia Augusto Righi, Universitdegli Studi di Bologna, Via Gobetti 93/2, I-40129 Bologna, Italy*

Accepted 2023 July 19. Received 2023 June 29; in original form 2023 May 18

ABSTRACT

Young and intermediate-age star clusters of both Magellanic Clouds exhibit complex colour–magnitude diagrams. In addition to the extended main-sequence turn-offs (eMSTOs), commonly observed in star clusters younger than ∼2 Gyr, the clusters younger than ∼800 Myr exhibit split main sequences (MSs). These comprise a blue MS, composed of stars with low rotation rates, and a red MS, which hosts fast-rotating stars. While it is widely accepted that stellar populations with different rotation rates are responsible for the eMSTOs and split MSs, their formation and evolution are still debated. A recent investigation of the ∼1.7-Gyr-old cluster NGC 1783 detected a group of eMSTO stars extremely dim in ultraviolet (UV) bands. Here, we use multiband *Hubble Space Telescope* photometry to investigate five star clusters younger than ∼200 Myr, including NGC 1805, NGC 1818, NGC 1850, and NGC 2164 in the Large Magellanic Cloud, and the Small Magellanic Cloud cluster NGC 330. We discover a group of bright MS stars in each cluster that are significantly dim in the *F*225*W* and *F*275*W* bands, similar to what is observed in NGC 1783. Our result suggests that UV-dim stars are common in young clusters. The evidence that most of them populate the blue MS indicates that they are slow rotators. As a by-product, we show that the star clusters NGC 1850 and BHRT 5b exhibit different proper motions, thus corroborating the evidence that they are not gravitationally bound.

Key words: Hertzsprung–Russell and colour–magnitude diagrams – Magellanic Clouds – galaxies: star clusters: general.

1 INTRODUCTION

In recent years, the split main sequence (MS) has been discovered as a common feature of young cluster colour–magnitude diagrams (CMDs; Milone et al. 2015, 2023). High-precision photometry from *Hubble Space Telescope* (*HST*) images reveals that all Magellanic Cloud clusters younger than ∼800 Myr exhibit a blue MS, which comprises about one-third of MS stars, and a more populous red MS (e.g. Milone et al. 2018).

The blue MS consists of fast rotators, whereas blue MS stars exhibit small rotational velocities, as demonstrated by high-resolution spectra of MS stars (Marino et al. 2018a,b). These findings corroborate the conclusion based on isochrone fitting of the CMD that stellar rotation is the main responsible for the split MS (D'Antona et al. 2015).

Similarly, the extended main-sequence turn-off (eMSTO), a distinctive feature of star clusters younger than ∼2 Gyr (Mackey & Broby Nielsen 2007; Milone et al. 2009; Goudfrooij et al. 2011), is populated by stars with different rotation rates as early suggested by theoretical studies (Bastian & de Mink 2009; D'Antona et al. 2015; Georgy et al. 2019) and demonstrated by works based on spectroscopy (Dupree et al. 2017; Marino et al. 2018a,b). However, rotation alone does not seem enough to fully account for the observed eMSTO. Hence, it is possible that age variation provides a contribution (e.g. Goudfrooij, Girardi & Correnti 2017, but see Cordoni et al. 2022). Intriguingly, split or broadened MSs and eMSTOs have been observed in Galactic open clusters with the same ages (Cordoni et al. 2018; Marino et al. 2018a; Li et al. 2019).

The origin of multiple stellar populations with different rotation rates is still under debate. D'Antona et al. (2015, 2017) suggested that all stars are born as fast rotators and that some of them are braked during their MS lifetime due to interaction in binary systems. As an alternative, the different rotation velocities may be imprinted in the early time of cluster formation depending on the lifetime of protostellar discs in pre-MS stars. Specifically, present-day fast rotators are the progeny of pre-MS stars with short-lived protostellar discs, whereas long removal times for protostellar discs would result in slow rotators (Tailo et al. 2016; Bastian et al. 2020). Wang et al. (2022) suggested that the blue MS stars are slow rotators originating from stellar mergers. Their scenario predicts that red MS stars gain their mass by disc accretion, which leads to rapid rotation, whereas binary merger is responsible for the formation of the blue MS.

Recently, a new CMD feature has been discovered along the eMSTO of NGC 1783. In the first paper of this series, Milone et al. (2023) have detected a group of stars located on the red

★ E-mail: antonino.milone@unipd.it

side of the eMSTO in CMDs composed of ultraviolet (UV) filters (see also Milone & Marino 2022). These UV-dim stars, which comprise ∼7 per cent of the total number of eMSTO stars of NGC 1783, define a narrow sequence and have colours similar to the remaining eMSTO stars, when observed in optical CMDs.

The observed colours and magnitudes of UV-dim stars can be reproduced by assuming the presence of an edge-on absorption dust ring, associated with grain condensation at the periphery of the excretion disc expelled by fast-spinning stars (D'Antona et al. 2023).

In this scenario, the entire eMSTO could be composed of dusty stars, which would significantly affect previous conclusions on the role of age and rotation on the eMSTO (see D'Antona et al. 2023, for details).

Martocchia et al. (2023) have recently suggested that UV-dim stars are likely rapidly rotating stars. They associated the shell Be stars of the ∼100-Myr-old Large Magellanic Cloud (LMC) cluster NGC 1850 that are seen nearly equator-on with the UV-dim stars of this cluster.

In this work, we use multiband *HST* photometry to search for UV-dim stars in five Magellanic Cloud star clusters with ages between ∼10 and 200 Myr, namely NGC 330, NGC 1805, NGC 1818, NGC 1850, and NGC 2164.[1] These clusters, which are widely investigated in the context of multiple populations, exhibit split MSs, eMSTOs, and conspicuous populations of Be stars (Bastian et al. 2017; Correnti et al. 2017; Li et al. 2017; Marino et al. 2018a; Milone et al. 2018, 2023; Hastings et al. 2021; Cordoni et al. 2022). Our targets are the only young clusters with available photometry in the *F*225*W* or *F*275*W* band.

The paper is organized as follows. In Section 2, we describe the data and the data reduction. Section 3 is dedicated to the search for UV-dim stars in NGC 2164, which we use as a test case, whereas the remaining clusters are analysed in Section 4. Finally, the summary and the conclusions are provided in Section 5. As a by-product of our investigation, Appendix A presents the proper motions of the double cluster composed of NGC 1850 and BHRT 5b and of the LMC stars in their field of view.

2 DATA AND DATA ANALYSIS

To study the young clusters, we used the catalogues by Milone et al. (2023), which include astrometry and photometry of 113 Magellanic Cloud clusters derived from *HST* images. We used photometry in the *F*336*W* and *F*814*W* bands of the Ultraviolet and Visible Channel of the Wide Field Camera 3 (UVIS/WFC3) of all clusters. In addition, we used *F*225*W* UVIS/WFC3 photometry of NGC 330, NGC 1805, NGC 1818, and NGC 2164, and *F*275*W* UVIS/WFC3 photometry of NGC 1850. In addition, we reduced and analysed the UVIS/WFC3 images of NGC 1850 collected on 2021 September 21 as part of GO-16748 (PI: F. Niederhofer). These data, which consist of two 40 s images and five 350 s images observed through the *F*814*W* filter, are used to measure the proper motions of stars in the field of view of NGC 1850.

Stellar fluxes and positions are measured by Milone et al. (2023) with the KS2 computer program, which was developed by Jay Anderson as the evolution of the KITCHEN_SYNC (Anderson et al. 2008), originally written to reduce images collected with the Wide Field Channel of the Advanced Camera for Surveys onboard *HST*. In a nutshell, KS2 uses three methods to measure the stars, which derive the optimal astrometry and photometry for stars with different luminosities. Since we are interested in bright stars, we used the results obtained from method I. It measures all stellar sources that generate a distinct peak within a 5 × 5 pixel region after neighbour stars subtraction. To do this, KS2 calculates the flux and position of each star in each image, separately, by using the point spread function (PSF) model associated with its position and subtracting the sky level computed from the annulus between 4 and 8 pixels from the stellar centre. Finally, the results from all images are averaged together to obtain the best determinations of stellar magnitudes and positions. The KS2 computer program provides various diagnostics of the photometric quality. Since we are interested in high-precision photometry, we included in the analysis only isolated stars that are well fitted by the PSF model (see section 2.4 from Milone et al. 2023, for details). For NGC 1850, which is the only analysed cluster that is significantly affected by differential reddening, we used the magnitudes corrected for differential reddening provided by Milone et al. (2023). To derive the proper motions of stars in the field of view of NGC 1850, we followed the procedure by Milone et al. (2023, see their section 5). In a nutshell, we first derived proper motions relative to NGC 1850 by comparing the positions of stars at different epochs. Specifically, in addition to the GO-16748 images, we used UVIS/WFC3 images collected in *F*814*W* on 2015 October 22 as part of GO-14174, *F*438*W* images observed on 2015 December 19 (GO-14069), and *F*467M images taken on 2009 October 20 (GO-11925). Stellar positions are corrected for geometric distortion by using the solution provided by Bellini & Bedin (2009) and Bellini, Anderson & Bedin (2011). The proper motions are transformed from relative to absolute by using the stars for which both relative proper motions and absolute proper motions from the *Gaia* Data Release 3 (Gaia Collaboration 2023) are available (see Milone et al. 2023, for details on the data set and on the methods to estimate the proper motions).

The results are illustrated in Fig. 1, where we plot the proper motion diagrams for stars in the field of view of NGC 1850 in five *F*814*W* magnitude intervals. The proper motions allowed us to separate the majority of cluster members (black dots) from probable field stars (azure crosses). The red circles that enclose the bulk of cluster members are centred on the average motion of NGC 1850 $[(\mu_\alpha \cos\delta, \mu_\delta) = (1.973 \pm 0.026, 0.086 \pm 0.028)$ mas yr$^{-1}]$ and have radii equal to 2.5σ, where σ is the average between the σ-clipped dispersion values of $\mu_\alpha \cos\delta$ and μ_δ. The right-hand panel of Fig. 1 shows the m_{F814W} versus $m_{F336W} - m_{F814W}$ CMD of the selected cluster members and field stars.

To investigate each cluster, we analyse the stars within two circular regions defined by Milone et al. (2018) within the same UVIS/WFC3 field of view. They include the cluster field, which is centred on the cluster and is mostly populated by cluster members, and the reference field, which has the same area as the cluster field but is mostly populated by field stars. The latter, which is located in the outskirts of the UVIS/WFC3 field, is used to statistically estimate the contamination of field stars in the cluster field (see Milone et al. 2018, for details).

[1] According to Milone et al. (2018), who using the isochrones from the Geneva data base (Ekström et al. 2012, 2013; Mowlavi et al. 2012), the ages of the studied clusters span the range between ∼30 and 100 Myr. The isochrones from the Padova data base (Marigo et al. 2017) provide ages between ∼10 and 200 Myr (Milone et al. 2023). The latter value may represent an upper limit to the age of NGC 2164 and is derived by assuming that the colour broadening of eMSTO stars is entirely due to age variations. For simplicity, we indicate the value of 200 Myr as an upper limit for the age of the studied clusters.

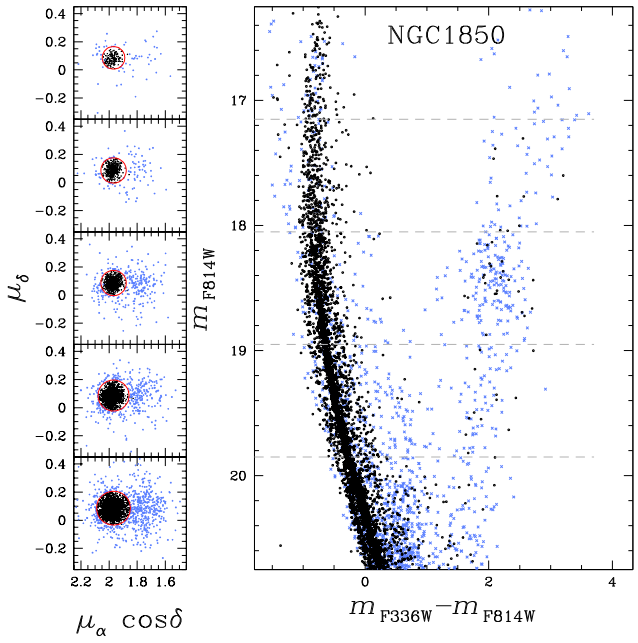

Figure 1. Proper motion diagram of stars in the field of view of NGC 1850 in 5 mag intervals (left). The right-hand panel shows the m_{F814W} versus $m_{F336W} - m_{F814W}$ CMD for stars with available proper motions. The probable cluster members (i.e. stars within the red circles of the left-hand panels) are coloured black, whereas the azure symbols represent the remaining stars.

2.1 Artificial stars

To estimate the photometric errors and generate the simulated CMD, we performed artificial star (AS) tests for each cluster. To do this, we followed the recipe by Anderson et al. (2008) and derived a list of 99 999 ASs with similar radial distributions and luminosity functions as the observed stars. The ASs have instrumental magnitudes[2] between the saturation limit of ~ -13.7 and -5.0 mag in the $F814W$ UVIS/WFC3 filter. The magnitudes in the other filters are derived from the fiducial lines of the red and blue MS. To derive the magnitudes and positions of the ASs we used the KS2 program and the same procedure that Milone et al. (2023) adopted for real stars. We included in our investigation only the relatively isolated ASs that are well fitted by the PSF and that we selected by using the same criteria adopted for the real stars.

3 UV-DIM STARS IN NGC 2164

To search for UV-dim stars in young clusters, we used the ∼200-Myr-old LMC cluster NGC 2164 as a test case. We first exploited the intermediate-age (∼1.7-Gyr-old) LMC cluster NGC 1783, where UV-dim stars have been discovered by Milone & Marino (2022) to constrain the properties of these stars in photometric diagrams constructed with optical and UV filters. Then, we extended the analysis to NGC 2164 and the other young clusters studied in this paper.

As illustrated in Fig. 2, the m_{F814W} versus $m_{F275W} - m_{F438W}$ CMD of NGC 1783 exhibits a cloud of stars with redder colours than the bulk of eMSTO stars. The most evident UV-dim stars, selected by Milone et al. (2023), are marked with magenta triangles. We plotted in the inset of Fig. 2 the $m_{F275W} - m_{F336W}$ versus $m_{F336W} - m_{F814W}$ two-colour diagram for the stars enclosed in the grey box. Clearly, UV-dim stars define a different sequence with respect to the remaining eMSTO stars, and exhibit redder $m_{F275W} - m_{F336W}$ colours than the bulk of eMSTO stars with similar $m_{F336W} - m_{F814W}$ values. Hence, this two-colour diagram is an efficient tool to identify the UV-dim stars.

The top-left panel of Fig. 3 shows the m_{F336W} versus $m_{F336W} - m_{F814W}$ CMD of NGC 2164 (Milone et al. 2023). The top-right panel provides a zoom around the CMD region where the split MS is more evident. From this diagram, we identified by eye the groups of blue and red MS stars and coloured them blue and red, respectively. The remaining stars, which are located on the red side of the MS and are coloured black, are probable binary systems composed of two MS stars. The blue and red lines are the fiducials of the two MSs. To derive the red fiducial, we considered 0.2 mag bins defined over a grid of points separated by steps of 0.05 mag (Silverman 1986). We computed the median of the colours and magnitudes of the red MS stars in each bin and smoothed the median points with the boxcar averaging method, which replaces each point with the average of the three adjacent points. We applied the same method for deriving the blue MS fiducial.

The middle panels show the m_{F336W} versus $m_{F225W} - m_{F336W}$ CMDs. As highlighted by the fiducial lines, blue and red MS stars exhibit similar colours. The $m_{F225W} - m_{F336W}$ colour separation is always smaller than ∼0.05 mag and the two sequences merge together around $m_{F336W} = 18.7$ mag, where blue MS stars span a wide colour range. For completeness, we used aqua-starred symbols to represent the Be stars identified by Milone et al. (2018), based on their flux excess in the $F656N$ band.

To further investigate the colour distribution of MS stars, we show in the bottom-left and bottom-middle panels of Fig. 3 the $m_{F225W} - m_{F336W}$ versus $m_{F336W} - m_{F814W}$ two-colour diagram for the NGC 2164 stars plotted in the top panels of Fig. 3. For simplicity, we only show MS and eMSTO stars brighter than $m_{F336W} = 21.0$, which is the magnitude level indicated by the dash–dotted lines in the top-left and middle-left panels.

The red MS defines a narrow sequence, similar to what is observed for the blue MS with $m_{F336W} - m_{F814W} \gtrsim -0.2$ mag. Conversely, the blue MS stars with $m_{F336W} - m_{F814W} \lesssim -0.2$ mag span a wide range of $m_{F225W} - m_{F336W}$ values. Specifically, we notice that about half of the blue MS stars only are superimposed on the red MS. The remaining blue MS stars (marked with open blue symbols in Fig. 3) exhibit larger $m_{F225W} - m_{F336W}$ values than red MS stars with the same $m_{F336W} - m_{F814W}$ colour, in close analogy with what is observed for UV-dim stars in NGC 1783. This subsample of blue MS stars, which we identify in the $m_{F225W} - m_{F336W}$ versus $m_{F336W} - m_{F814W}$ two-colour diagram, includes the most evident UV-dim stars (blue triangles), which exhibit the widest colour separation from the bulk of MS stars of more than 0.20 mag. The remaining UV-dim candidates with colour distances larger than 0.09 mag from the fiducial line of the bulk of MS stars are marked with blue diamonds. We notice that the UV candidates include four stars that, based on the position in the top-panel CMD, are binary systems composed of two MS stars (grey diamonds)[3] Intriguingly, the selected Be stars of NGC 2164 populate a narrow sequence and span the $m_{F336W} -$

[2]The instrumental magnitudes are defined as $-2.5 \log_{10}$ of the detected photoelectrons.

[3]We emphasize that $F438W$ data are not available for NGC 2164 and for most studied clusters, whereas photometry in the $F225W$ (or $F275W$), $F336W$, and $F814W$ is available for all of them. For this reason, we used the $m_{F225W} - m_{F336W}$ versus $m_{F336W} - m_{F814W}$ two-colour diagram to identify the candidate UV-dim stars.

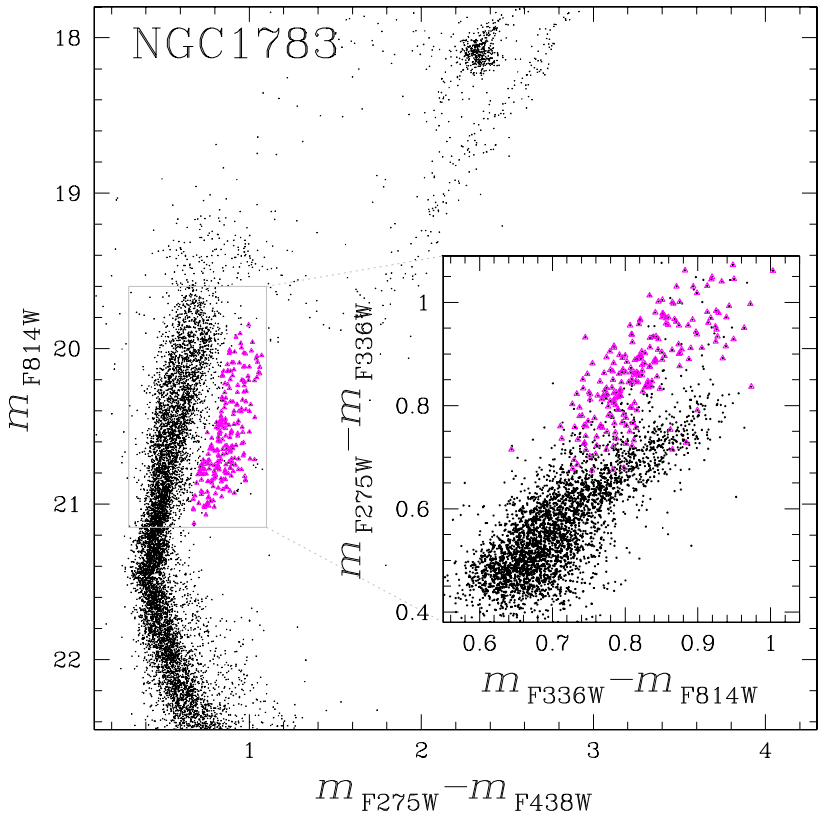

Figure 2. m_{F814W} versus $m_{F275W} - m_{F438W}$ CMD of the ∼1.7-Gyr-old LMC cluster NGC 1783. The inset shows the $m_{F275W} - m_{F336W}$ versus $m_{F336W} - m_{F814W}$ two-colour diagram for eMSTO stars. The UV-dim stars selected by Milone et al. (2023) are marked with magenta triangles.

m_{F814W} colour interval between ∼−0.9 and ∼−0.3 mag. Hence, they occupy a different region of the two-colour diagram with respect to the UV-dim stars.

A possible explanation is a consequence of the fact that the upper MS (i.e. the MS region populated by UV-dim stars) exhibits different slopes in the CMDs, and in the two-colour diagrams of young clusters and intermediate-age clusters. Specifically, the upper MS of the intermediate-age cluster NGC1783 (black stars in the inset of Fig. 2) has a positive slope in the two-colour diagrams, whereas the upper MS of NGC2164 and the other young clusters have negative slopes (e.g. bottom-left panels of Fig. 3 for NGC2164). Such slopes are consistent with those predicted by the isochrones (e.g. Fig. 4).

To estimate the contamination from field stars in the two-colour diagram of NGC 2164, we analyse the same diagram for stars in the reference field. The results are illustrated in the bottom-right panel of Fig. 3, where the blue and red colours represent the stars that occupy the regions of the m_{F336W} versus $m_{F336W} - m_{F814W}$ CMD, where we identified blue and red MS stars. The lack of reference-field stars in the portion of the two-colour diagram populated by candidate UV-dim stars indicates negligible contamination from field stars.

3.1 Comparison with simulated photometry

We used the Geneva models (Ekström et al. 2012, 2013; Mowlavi et al. 2012) to simulate the photometric diagrams for two distinct stellar populations with the same age, in close analogy with what we did in previous work (e.g. D'Antona et al. 2015; Milone et al. 2023). The simulated populations comprise 25 per cent of non-rotating stars, whereas the remaining stars have rotation rates corresponding to 0.9 times the critical value, which are the rotation values that provide the best match between the Geneva models and the split MSs of NGC 2164 (Milone et al. 2018) Similarly, the adopted ages (100 Myr) and the fractions of non-rotating stars are comparable with those of NGC 2164 (Milone et al. 2018).

We adopted random viewing-angle distributions, the gravity-darkening model by Espinosa Lara & Rieutord (2011), and the limb-darkening effect (Claret 2000). Finally, we derived the magnitudes into the *F*225*W*, *F*275*W*, *F*336*W*, and *F*814*W* bands of UVIS/WFC3 by means of the model atmospheres by Castelli (2005). We adopted for the simulated stars the same photometric errors derived from ASs with similar magnitudes and radial distances from the cluster centre.

The results are illustrated in Fig. 4, where we show the simulated m_{F336W} versus $m_{F336W} - m_{F814W}$ CMD and the $m_{F225W} - m_{F336W}$ versus $m_{F336W} - m_{F814W}$ two-colour diagram for bright MS stars. The simulated stellar populations overlap with each other in the two-colour diagram. Similar conclusions are obtained from the simulation of 20- and 200-Myr-old clusters and by assuming rotation rates equal to 0.6 times the critical value. These results indicate that the $m_{F225W} - m_{F336W}$ colour excess of the candidate UV-dim stars is due neither to observational errors nor to stellar rotation.

Noticeably, a visual inspection of Figs 2 and 3 reveals that the UV-dim stars of NGC 1783 and NGC 2164 occupy different regions of the two-colour diagrams. The difference is possibly a consequence of the fact that the upper MS exhibits different slopes in the two-colour diagrams of young clusters and intermediate-age clusters. Specifically, the upper MS of the intermediate-age cluster NGC 1783 (black stars in the inset of Fig. 2) has a positive slope in the two-colour diagrams, whereas the upper MS of NGC 2164 exhibits a

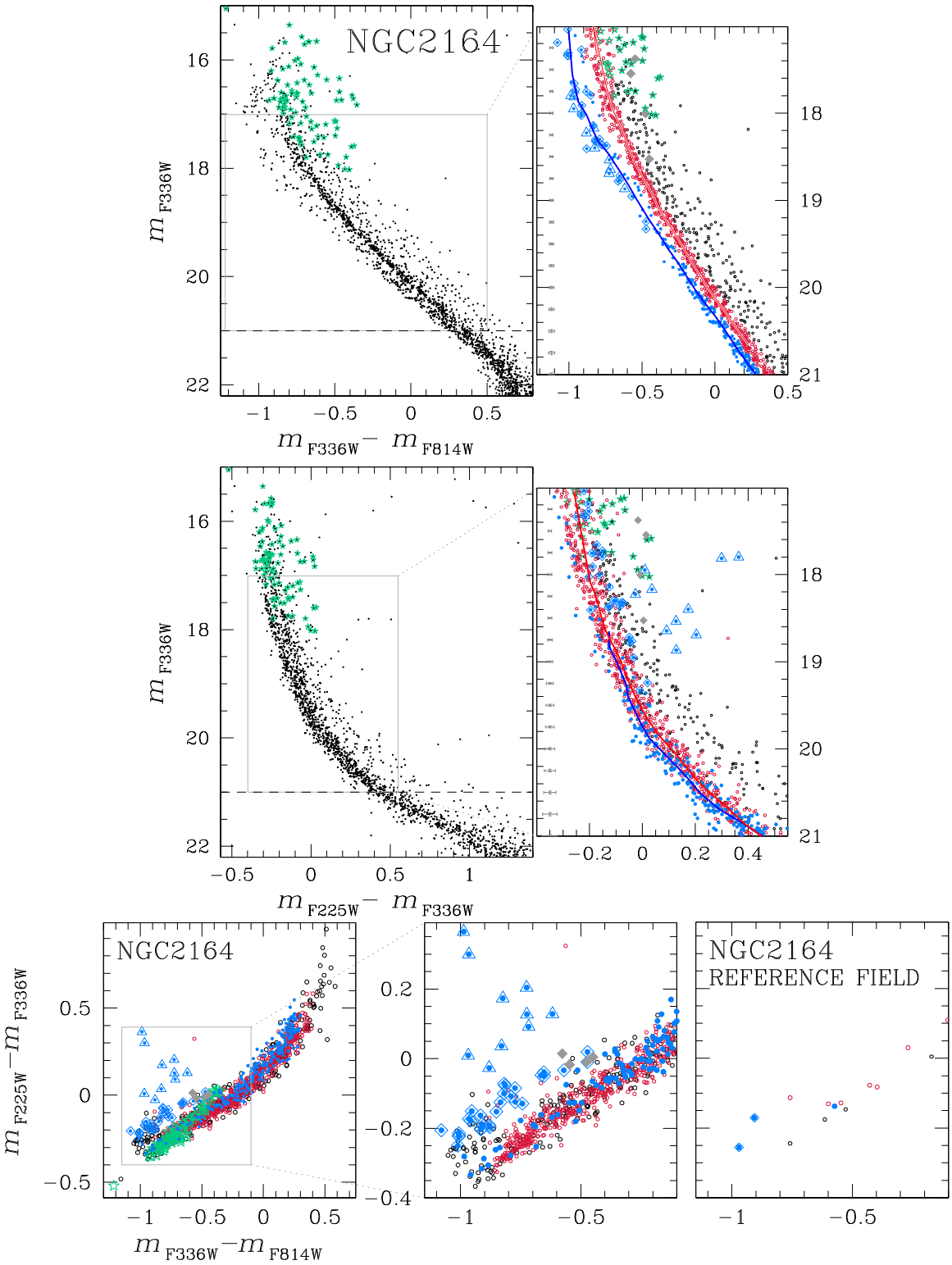

Figure 3. m_{F336W} versus $m_{F336W} - m_{F814W}$ (top) and m_{F336W} versus $m_{F225W} - m_{F336W}$ (middle) CMDs of stars in the cluster field of NGC 2164. The right-hand panels are zooms around the upper MS. The fiducial lines of the red and blue MSs are represented with red and blue lines, respectively. The bottom-left and bottom-middle panels show the $m_{F225W} - m_{F336W}$ versus $m_{F336W} - m_{F814W}$ two-colour diagrams for NGC 2164. Red and blue symbols indicate red and blue MS stars, respectively, selected from the top panel CMDs. The Be stars identified by Milone et al. (2018) are represented with aqua-starred symbols, whereas the candidate UV-dim stars are marked with blue diamonds and triangles. Grey diamonds represent probable UV-dim stars that, based on the position in the top-right CMD, are probable binaries. The bottom-left panel represents all the stars, while the bottom-middle panel is a zoom around the bright MS. For clearness, we excluded the Be stars from the bottom-middle panel plot. The $m_{F225W} - m_{F336W}$ versus $m_{F336W} - m_{F814W}$ two-colour diagram for stars in the reference field of NGC 2164 is plotted in the bottom-right panel.

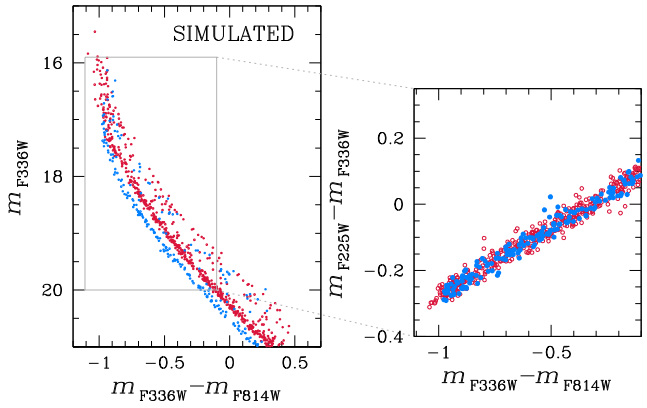

Figure 4. m_{F336W} versus $m_{F336W} - m_{F814W}$ simulated CMD for a 100-Myr-old cluster (left-hand panel). The $m_{F225W} - m_{F336W}$ versus $m_{F336W} - m_{F814W}$ diagram for the MS stars shown in the CMD inset is plotted in the right-hand panel.

negative slope, as predicted by the simulated diagrams of Fig. 4. Since the UV-dim stars have low fluxes in the *F225W* and *F275W* bands, compared with the remaining stars at similar evolutionary stage, they have larger *F225W* − *F336W* (or *F275W* − *F336W*) colours than the bulk of MS stars. Hence, the UV-dim stars populate the top-right part of the two-colour diagram in the intermediate-age cluster NGC 1783 but the top-left region of the diagrams of the young cluster NGC 2164.

4 UV-DIM STARS IN YOUNG CLUSTERS

To search for UV-dim stars in the other young clusters with available *F225W* or *F275W* photometry, we extended the analysis of Section 3 to the LMC clusters NGC 1850, NGC 1805, and NGC 1818, and to the Small Magellanic Cloud (SMC) cluster NGC 330. The results are illustrated in Figs 5 and 6, where we show the $m_{F225W} - m_{F336W}$ (or $m_{F275W} - m_{F336W}$) versus $m_{F336W} - m_{F814W}$ two-colour diagrams for stars in the cluster field (left-hand and middle panels) and in the reference field (right-hand panels).

Similar to what is observed for NGC 2164, the red MS stars of these four clusters, which are identified from the m_{F336W} versus $m_{F336W} - m_{F814W}$ CMD, define narrow sequences in the two-colour diagrams of Figs 5 and 6. Conversely, the blue MS stars with $m_{F336W} - m_{F814W} \lesssim -0.2$ mag are spread over a wide area of the two-colour diagram and exhibit larger $m_{F225W} - m_{F336W}$ values than the majority of MS stars with similar $m_{F336W} - m_{F814W}$ colours. A visual comparison between the two-colour diagrams of stars in the cluster and reference fields shows that contamination from field stars is negligible in all clusters. We conclude that UV-dim stars are common features in the CMDs of clusters younger than ∼200 Myr.

Intriguingly, the Be stars of the different clusters exhibit different behaviours in the two-colour diagrams. While nearly all Be stars of NGC 2164 and NGC 1850 define narrow sequences in the $m_{F225W} - m_{F336W}$ (or $m_{F275W} - m_{F336W}$) versus $m_{F336W} - m_{F814W}$ two-colour diagrams, several Be stars of NGC 1805, NGC 330, and NGC 1818 exhibit a large star-to-star colour scatter.

5 SUMMARY AND DISCUSSION

We analysed UVIS/WFC3 photometry of five Magellanic Cloud clusters younger than ∼200 Myr in the *F225W* (or *F275W*), *F336W*, and *F814W* bands. We also used *F656N* photometry to identify Be stars. We discovered that a significant fraction of their bright blue MS stars exhibit larger $m_{F225W} - m_{F336W}$ colours than the bulk of MS stars, in close analogy with what we observed for UV-dim stars in NGC 1783. The colours of these stars are not consistent with the colours of stellar populations with different rotation rates that we simulated by using the Geneva models (Ekström et al. 2012, 2013). We conclude that UV-dim stars are not a peculiarity of the ∼1.7-Gyr-old star cluster NGC 1783 but are common features of young Magellanic Cloud clusters. Intriguingly, most of the UV-dim stars detected in young clusters populate the bright portion of the blue MS, which is composed of slow-rotating stars (D'Antona et al. 2015; Marino et al. 2018a).

In a recent paper, Martocchia et al. (2023) analysed optical and UV photometry of NGC 1850 and suggested that the rapidly rotating Be stars of this cluster, previously identified by Kamann et al. (2023) by using the Multi-Unit Spectroscopic Explorer (MUSE) spectra, correspond to the UV-dim stars. They concluded that UV-dim stars are possibly rapidly rotating stars, which are seen nearly equator-on and thus are extinct by their own decretion discs.

Our investigation does not exclude the connection between UV-dim stars and Be stars suggested by these authors. Nevertheless, since all UV-dim stars that we identified in NGC 1850 do not exhibit Hα emission, they do not correspond to the sample of UV-dim stars by Martocchia and collaborators. A significant difference between the bulk of Be stars and the selected UV-dim stars is that they populate distinct regions of the $m_{F225W} - m_{F336W}$ (or $m_{F275W} - m_{F336W}$) versus $m_{F336W} - m_{F814W}$ two-colour diagrams. Specifically, while Be and UV-dim stars share a similar interval of $m_{F336W} - m_{F814W}$, the majority of UV-dim stars are spread over a wide interval of $m_{F225W} - m_{F336W}$.

The physical mechanisms that are responsible for the UV-dim stars are investigated by D'Antona et al. (2023) who compared the observed CMDs of NGC 1783 stars with simulated photometry by assuming that some stars are obscured by dust. Since the amount of absorption due to dust depends on the wavelength, they reproduced the colours of UV-dim stars by assuming that the dust is distributed in a ring and the stars are seen nearly equator-on. D'Antona and collaborators suggested that circumstellar dust is associated with mass-loss events that can preferentially occur in fast-rotating stars.

The fact that the UV-dim stars in young clusters are slow rotators could be a challenge for the scenario by D'Antona et al. (2023). However, as proposed by D'Antona et al. (2017), the blue MSs of young clusters may be composed of stars initially rapidly rotating, but that have later slowed down. In this context, we may speculate that the UV-dim stars of the young clusters are indeed stars that have been recently subject to an intense mass-loss event. This event caused both their abnormal UV absorption and braked their rotation, shifting the star location to the slow-rotating MS (Dell'Agli et al., in preparation). Alternatively, if the blue MS is due to merging (Wang et al. 2022), we suggest that the merging event has been recent enough that the strong UV absorption is caused by the remnant circumstellar debris of this event.

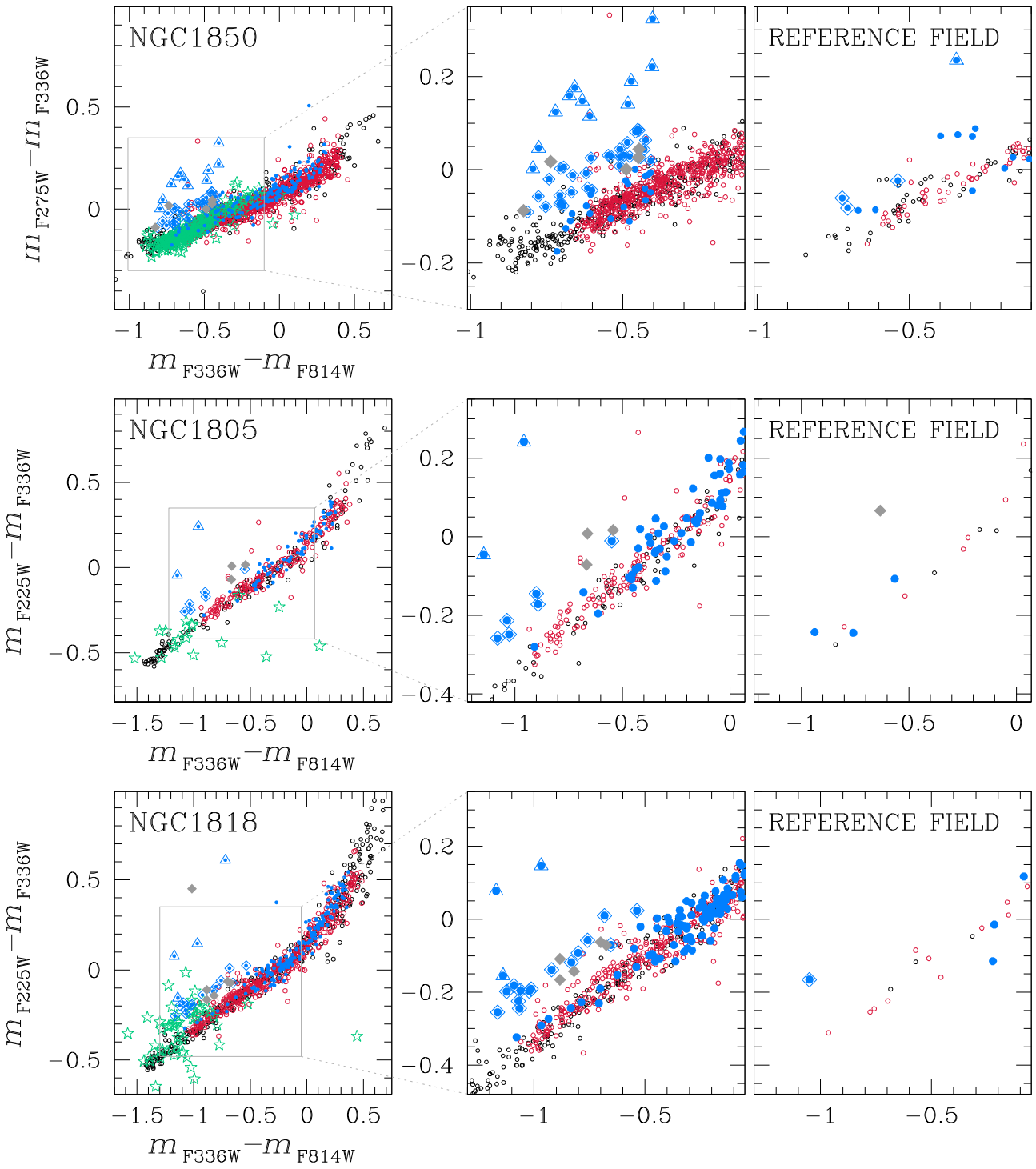

Figure 5. $m_{F275W} - m_{F336W}$ ($m_{F225W} - m_{F336W}$) versus $m_{F336W} - m_{F814W}$ two-colour diagrams for stars in the cluster fields of the LMC clusters NGC 1850, NGC 1805, and NGC 1818 (right-hand panels). The middle panels are zooms of the right-hand panel diagrams for stars in the upper MS. The two-colour diagrams plotted in the right-hand panels show the stars in the reference field. The symbols and colours are the same as in Fig. 3. For clearness, in the middle and right-hand panels, we excluded the Be stars.

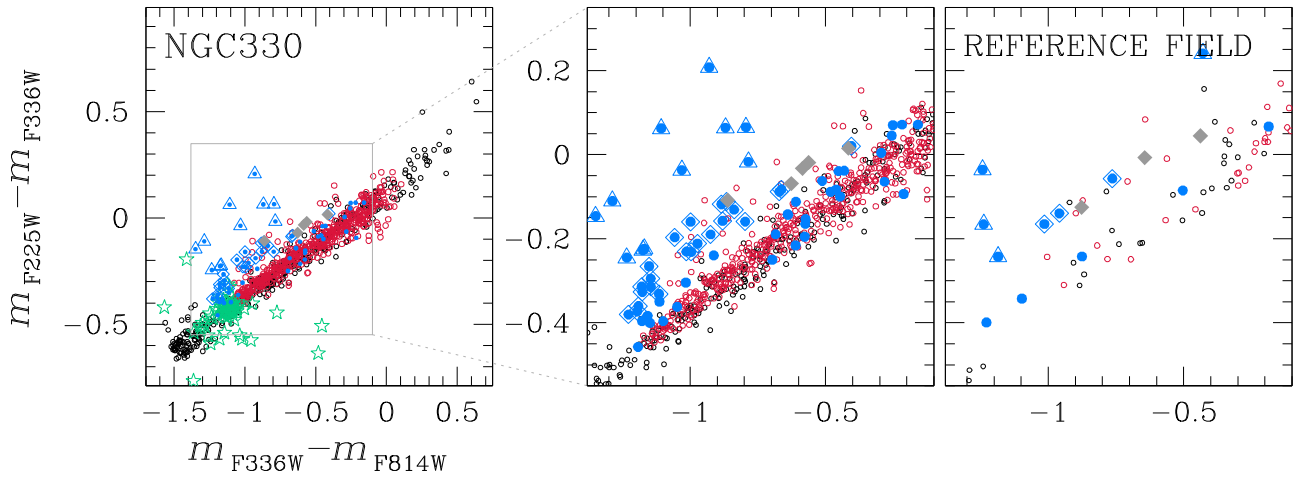

Figure 6. As in the Fig. 5, but for the SMC cluster NGC 330.

ACKNOWLEDGEMENTS

We thank the referee for improving the paper. This work has received funding from the European Union's Horizon 2020 research and innovation programme under the Marie Sklodowska-Curie Grant Agreement No. 101034319 and from the European Union – NextGenerationEU, beneficiary: TZ. APM, GC, AFM, FD'Antona, FDell'Agli, and PV acknowledge the support received from INAF Research GTO-Grant Normal RSN2-1.05.12.05.10 – Understanding the formation of globular clusters with their multiple stellar generations (ref. AFM) of the 'Bando INAF per il Finanziamento della Ricerca Fondamentale 2022'.

DATA AVAILABILITY

The data underlying this paper will be shared upon reasonable request to the corresponding author.

REFERENCES

Anderson J. et al., 2008, AJ, 135, 2055
Bastian N., de Mink S. E., 2009, MNRAS, 398, L11
Bastian N. et al., 2017, MNRAS, 465, 4795
Bastian N., Kamann S., Amard L., Charbonnel C., Haemmerlé L., Matt S. P., 2020, MNRAS, 495, 1978
Bellini A., Bedin L. R., 2009, PASP, 121, 1419
Bellini A., Anderson J., Bedin L. R., 2011, PASP, 123, 622
Castelli F., 2005, Mem. Soc. Astron. Ital. Suppl., 8, 25
Claret A., 2000, A&A, 363, 1081
Cordoni G., Milone A. P., Marino A. F., Di Criscienzo M., D'Antona F., Dotter A., Lagioia E. P., Tailo M., 2018, ApJ, 869, 139
Cordoni G. et al., 2022, Nat. Commun., 13, 4325
Correnti M., Goudfrooij P., Bellini A., Kalirai J. S., Puzia T. H., 2017, MNRAS, 467, 3628
D'Antona F., Di Criscienzo M., Decressin T., Milone A. P., Vesperini E., Ventura P., 2015, MNRAS, 453, 2637
D'Antona F., Milone A. P., Tailo M., Ventura P., Vesperini E., di Criscienzo M., 2017, Nat. Astron., 1, 0186
D'Antona F. et al., 2023, MNRAS, 521, 4462
Dias B. et al., 2021, A&A, 647, L9
Dupree A. K. et al., 2017, ApJ, 846, L1
Ekström S. et al., 2012, A&A, 537, A146
Ekström A. et al., 2013, Phys. Rev. Lett., 110, 192502
Espinosa Lara F., Rieutord M., 2011, A&A, 533, A43
Gaia Collaboration, 2023, A&A, 674, A1
Georgy C. et al., 2019, A&A, 622, A66
Goudfrooij P., Puzia T. H., Chandar R., Kozhurina-Platais V., 2011, ApJ, 737, 4
Goudfrooij P., Girardi L., Correnti M., 2017, ApJ, 846, 22
Hastings B., Langer N., Wang C., Schootemeijer A., Milone A. P., 2021, A&A, 653, A144
Kamann S. et al., 2023, MNRAS, 518, 1505
Li C., de Grijs R., Deng L., Milone A. P., 2017, ApJ, 844, 119
Li C., Sun W., de Grijs R., Deng L., Wang K., Cordoni G., Milone A. P., 2019, ApJ, 876, 65
Mackey A. D., Broby Nielsen P., 2007, MNRAS, 379, 151
Marigo P. et al., 2017, ApJ, 835, 77
Marino A. F., Przybilla N., Milone A. P., Da Costa G., D'Antona F., Dotter A., Dupree A., 2018a, AJ, 156, 116
Marino A. F., Milone A. P., Casagrande L., Przybilla N., Balaguer-Núñez L., Di Criscienzo M., Serenelli A., Vilardell F., 2018b, ApJ, 863, L33
Martocchia S., Bastian N., Saracino S., Kamann S., 2023, MNRAS, 520, 4080
Milone A. P., Marino A. F., 2022, Universe, 8, 359
Milone A. P., Bedin L. R., Piotto G., Anderson J., 2009, A&A, 497, 755
Milone A. P. et al., 2015, MNRAS, 450, 3750
Milone A. P. et al., 2018, MNRAS, 477, 2640
Milone A. P. et al., 2023, A&A, 672, A161
Mowlavi N., Eggenberger P., Meynet G., Ekström S., Georgy C., Maeder A., Charbonnel C., Eyer L., 2012, A&A, 541, A41
Piatti A. E., 2021, A&A, 650, A52
Schmidt T. et al., 2022, A&A, 663, A107
Silverman B. W., 1986, Density Estimation for Statistics and Data Analysis. Chapman and Hall, London
Sollima A., D'Orazi V., Gratton R., Carini R., Carretta E., Bragaglia A., Lucatello S., 2022, A&A, 661, A69
Tailo M., Di Criscienzo M., D'Antona F., Caloi V., Ventura P., 2016, MNRAS, 457, 4525
Wang C. et al., 2022, Nat. Astron., 6, 480
Zivick P. et al., 2018, ApJ, 864, 55

APPENDIX A: PROPER MOTIONS OF THE STAR CLUSTER BHRT 5B AND OF LMC STARS

In Section 2, we derived the proper motions of stars in the direction of NGC 1850 and used them to separate the bulk of cluster members from field stars. In the following, we use these proper motions to

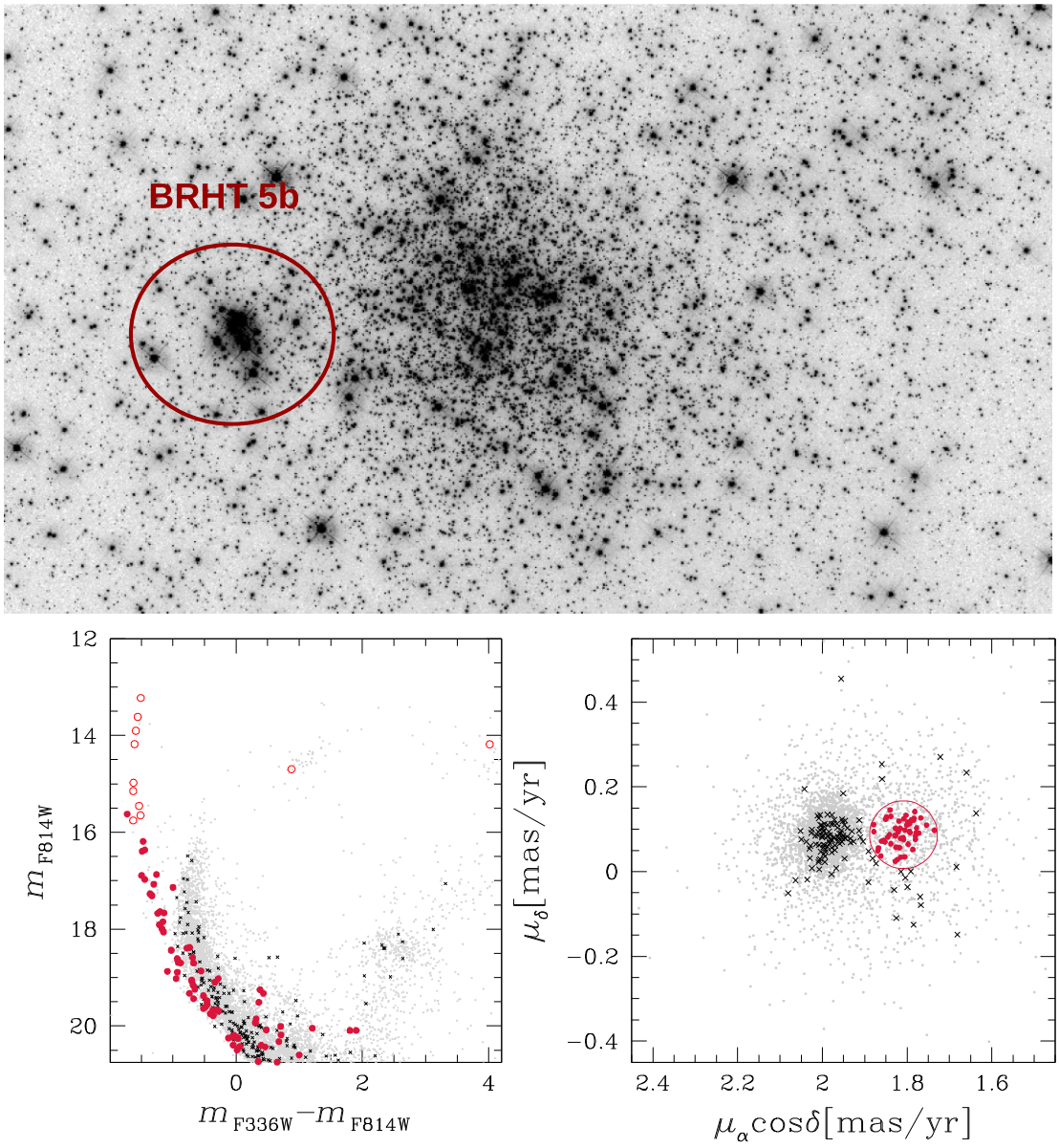

Figure A1. Stacked *F*467M UVIS/WFC3 image of the star clusters NGC 1850 and BRHT 5b (top). The bottom panels show the m_{F814W} versus $m_{F336W} - m_{F814W}$ CMD (left) and the proper motion diagram (right) of stars in the field of view of NGC 1850. The crimson-filled dots show the probable BRHT 5b members that are located within the crimson circle shown in the top panel and that we selected from the proper motion diagram. The remaining stars with a distance smaller than 12 arcsec from the centre of BRHT 5b, and available proper motions are represented with black crosses. The stars within 12 arcsec from the cluster centre and without proper motions are plotted with open circles.

better constrain the kinematics of the stellar populations in the field of view.

As shown in the top panel of Fig. A1, where we plot the stacked *F*467M UVIS/WFC3 image of stars around NGC 1850, a distinctive feature of this cluster is the presence of BHRT 5b, which is a compact cluster ∼30 arcsec west from its centre. Because of the small projected distance between these two clusters, NGC 1850 is considered a double cluster, but the possibility that the two clusters are gravitationally bound is still debated (e.g. Sollima et al. 2022, and references therein).

To investigate the proper motion of BHRT 5b, we selected the stars within the crimson circle plotted in the bottom panel of Fig. A1, which is centred on BHRT 5b and has a radius of 12 arcsec. These stars are plotted with coloured symbols in the CMD and proper motion diagrams of the lower panels.

As shown in the bottom-right panel of Fig. A1, most of the selected stars are clustered into two regions of the proper motion diagram. Some stars share the same proper motions of NGC 1850 and have similar colours and magnitudes thus indicating that they are probable members of this cluster. Conversely, the group of stars that we associate with BHRT 5b is clustered around $(\mu_\alpha \cos\delta, \mu_\delta) = (1.822 \pm 0.008 \pm 0.026, 0.087 \pm 0.007 \pm 0.028)$ mas yr^{-1}. Here, the two error components indicate the uncertainty on the proper motion relative to NGC 1850 and the error on the absolute

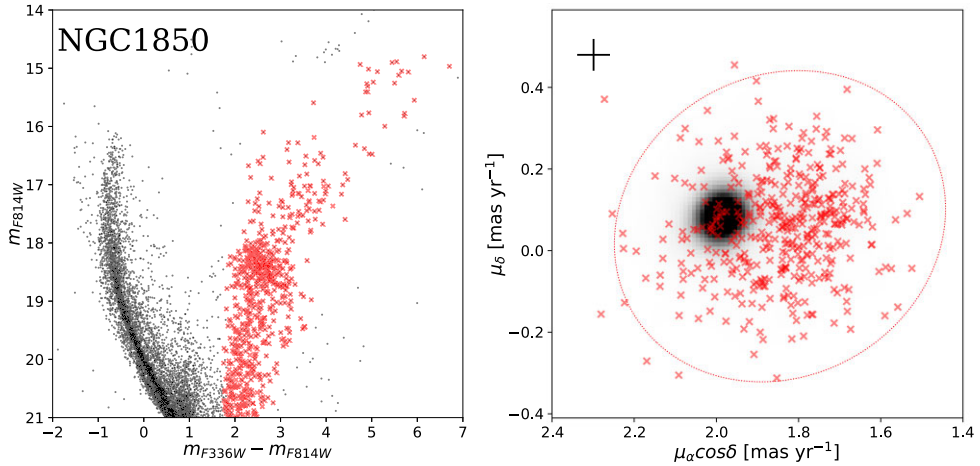

Figure A2. m_{F814W} versus $m_{F336W} - m_{F814W}$ CMD (left) and proper motion diagram of stars in the field of view of NGC 1850 (right). The LMC RGB stars are marked with red crosses, while the red ellipse provides the best fitting of the proper motion distribution of RGB stars.

proper motion of NGC 1850. To select the probable members of BHRT 5b in the proper motion diagram, we iteratively defined a circle centred on the BHRT 5b average motion and with a radius of 0.08 mas yr^{-1}, which corresponds to three times the average proper motion uncertainty. The fact that these stars, which are coloured with crimson-filled dots, populate the brightest MS portion of the CMD corroborates the evidence that they belong to BHRT 5b. We conclude that, due to the different proper motions, NGC 1850 and BHRT 5b are not gravitationally bound.

In addition to constraining the kinematics of star clusters, the stellar proper motions allow us to characterize the stellar populations of the LMC. To do that, we used the CMD plotted in left-hand panel of Fig. A2 to identify the LMC red giant branch (RGB) stars in the field of view of NGC 1850 (red crosses). As shown in the right-hand panel of Fig. A2, the selected LMC stars have a median proper motion $(\mu_\alpha \cos\delta,\ \mu_\delta) = (1.831 \pm 0.006 \pm 0.026,\ 0.065 \pm 0.006 \pm 0.028)$ mas yr^{-1} and exhibit a nearly circular distribution. Specifically, the ellipse that provides the best fit with the observed proper motion distribution has ellipticity, $\epsilon = 0.10 \pm 0.07$, and position angle, $\theta = 37 \pm 12^\circ$.[4]

The evidence that the old LMC stars in the background and foreground NGC 1850 exhibit nearly circular distributions is consistent with the findings by Milone et al. (2023) based on LMC stars in the field of views of NGC 1755, NGC 1801, and NGC 1953. In contrast, the behaviour of the proper motions of old LMC stars is different from what observed for both young and old SMC stars, whose proper motions exhibit high ellipticity values and major axes that point toward the LMC (Zivick et al. 2018; Dias et al. 2021; Piatti 2021; Schmidt et al. 2022; Milone et al. 2023).

[4]We considered the ellipse that encloses 90 per cent of stars, and defined the ellipticity $\epsilon = 1 - b/a$, where a and b are the minor and major axes of the ellipse (see Milone et al. 2023, for details).

This paper has been typeset from a TEX/LATEX file prepared by the author.